Inorganic Chemistry

Article

pubs.acs.org/IC

Design and Synthesis of a Luminescent Cyclometalated Iridium(III) Complex Having *N*,*N*-Diethylamino Group that Stains Acidic Intracellular Organelles and Induces Cell Death by Photoirradiation

Shinsuke Moromizato,[†] Yosuke Hisamatsu,[†,‡] Toshihiro Suzuki,[‡,§] Yasuki Matsuo,[†] Ryo Abe,[‡,§] and Shin Aoki*[,†,‡]

[†]Faculty of Pharmaceutical Sciences, [‡]Center for Technologies against Cancer (CTC), and [§]Research Institute for Biomedical Sciences, Tokyo University of Science, 2641 Yamazaki, Noda, Chiba, 278-8510 Japan

Supporting Information

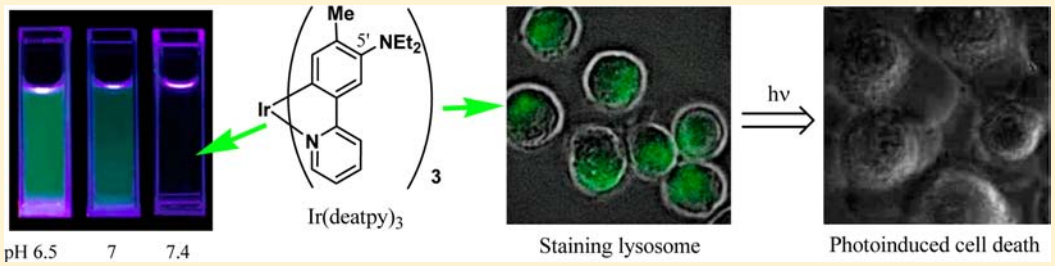

ABSTRACT: Cyclometalated iridium(III) complexes have received considerable attention and are important candidates for use as luminescent probes for cellular imaging because of their potential photophysical properties. We previously reported that *fac*-Ir(atpy)$_3$ **4** (atpy = 2-(5′-amino-4′-tolyl)pyridine) containing three amino groups at the 5′-position of the atpy ligand shows a maximum red emission (at around 600 nm) under neutral and basic conditions and a green emission (at 531 nm) at acidic pH (pH 3−4). In this Article, we report on the design and synthesis of a new pH-sensitive cyclometalated Ir(III) complex containing a 2-(5′-*N*,*N*-diethylamino-4′-tolyl)pyridine (deatpy) ligand, *fac*-Ir(deatpy)$_3$ **5**. The complex exhibits a considerable change in emission intensity between neutral and slightly acidic pH (pH 6.5−7.4). Luminescence microscopic studies using HeLa-S3 cells indicate that **5** can be used to selectively stain lysosome, an acidic organelle in cells. Moreover, complex **5** is capable of generating singlet oxygen in a pH-dependent manner and inducing the death of HeLa-S3 cells upon photoirradiation at 377 or 470 nm.

INTRODUCTION

The pH-responsive probes have played important roles in bioimaging studies of organelles, cells, and tissues. It is well-known that the pH of some organelles such as the golgi apparatus, endosomes, and lysosomes are 6.7, 6.5, and 5.5, values[1] that are lower than the pH of the cytosol and mitochondria (7.2−7.5) in normal cells.[2] In addition, it has been reported that the pH of some types of cancer tissues are in the slightly acidic range, that is, below 7.[3] Many examples of intracellular pH probes have been reported to date.[4] For example, LysoSensor, Blue DND-167, and SNARF-5F are commercially available for pH probes.[4,5] However, there are a few examples of reversible on−off pH-probes that respond to changes in intracellular pH. Urano's group and Overkleeft's group reported on pH-dependent on−off fluorescent probes that contain aniline moieties at the *meso* position of BODIPY, the pK_a values of which can be tuned by inserting the appropriate alkyl substituents on the aniline nitrogen.[6]

Phosphorescent heavy-metal complexes have been subjects of considerable attention because of their unique photophysical properties. High-luminescence quantum yields offer high sensitivity, relatively long lifetimes (τ ~μs) that eliminate the short-lived autofluorescence (τ ~ns) from biological samples,[7] and significant Stokes shift that minimize the self-quenching process. Cyclometalated iridium(III) complexes[8] such as *fac*-Ir(ppy)$_3$ **1** (ppy = 2-phenylpyridine) and *fac*-Ir(tpy)$_3$ **2** (tpy = 2-(4′-tolylpyridine), (Chart 1) are representative scaffolds for phosphorescent emitters in organic light-emitting diodes (OLEDs),[9] oxygen sensors,[10] chemosensors,[11] and luminescent probes for biological systems[12] including proteins,[13] and DNA.[14] Moreover, several cyclometalated iridium(III) complexes have been reported as cellular imaging probes for the

Chart 1

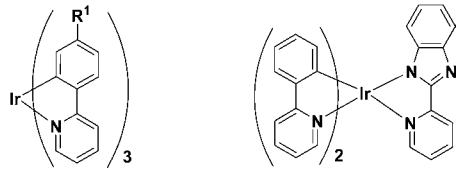

1: R^1 = H (*fac*-Ir(ppy)$_3$)
2: R^1 = Me (*fac*-Ir(tpy)$_3$)

Williams's Ir complex
3: Ir(ppy)$_2$(pybz)

Received: June 20, 2012
Published: November 12, 2012

detection of nucleoli,[14a,15] golgi apparatus,[14b] cytoplasm,[16] perinuclear materials,[17] lysosomes,[18] intracellular metal ions,[19] and low oxygen concentration regions of tumor tissues.[20,21] Regarding pH probes that are sensitive to a change in intracellular pH, an Ir complex having a 2-pyridyl-benzimidazole ligand ($Ir(ppy)_2(pybz)$ **3** (Chart 1)), when protonated, undergoes a change in its emission wavelength (a change of ca. 80 nm), which permits it to be used to selectively stain lysosomes.[18a]

Meanwhile, photodynamic therapy (PDT)[22] is one of the potent methodologies for the treatment of various tumors by singlet oxygen ($^1O_2$) that is generated from triplet oxygen ($^3O_2$) by the photoactivation of photosensitizers such as porphyrins, phthalocyanines, methylene blue, BODIPY, and so on.[23] Regarding such Ir complexes, several groups reported that bis- and tris-cyclometalated Ir(III) complexes can function as efficient sensitizers for producing $^1O_2$.[24] It has been reported that the efficiency of $^1O_2$ generation of some photosensitizers such as methylene blue are dependent on the pH of the solution.[25] Despite these efforts, to the best of our knowledge, metal complexes that have dual functions as luminescence pH-sensors and pH-dependent photosensitizers in living cells have not been developed.

We recently reported the regioselective halogenation, nitration, and formylation of **1** and **2** at the 5′-position (*para* to the C−Ir bond) of the phenyl ring, and their subsequent conversion to formyl, cyano, sulfonyl, and amino groups, which afford unique Ir complexes.[26−28] As shown in Chart 2, acid-free

Chart 2

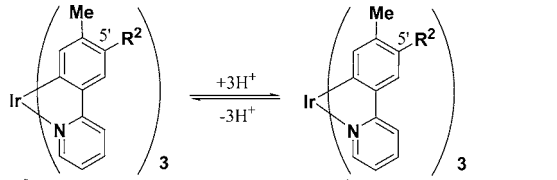

fac-$Ir(atpy)_3$ **4** (atpy = 2-(5′-amino-4′-tolyl)pyridine), which contains three amino groups at the 5′-position exhibits a weak red colored luminescence emission at 613 nm in dimethylsulfoxide (DMSO), which is a much longer wavelength than that of **2** (green emission at 513 nm), and the emission color of **4** in aqueous solution is dependent on the pH of the solution.[26] The red colored emission of **4** (at around 600 nm) under neutral~basic conditions changes to a green emission (at around 530 nm) under acidic conditions (at pH 3−4), because its electron-donating NH_2 group becomes an electron-withdrawing $(NH_3)^+$ group upon protonation.

In this Article, we report on the preparation of a new pH-sensitive Ir(III) complex that contains three *N*,*N*-diethylamino groups, *fac*-$Ir(deatpy)_3$ **5** (deatpy = 2-(5′-*N*,*N*-diethylamino-4′-tolyl)pyridine) (Chart 2). Prior to the synthesis of **5**, its pK_a values were predicted to be about 7 based on the pK_a values of known *N*,*N*-dialkylaniline derivatives. As expected, the emission of **5** was almost silent at pH 7.4, and a strong green luminescence emission was observed at pH <7, due to the protonation of diethylamino groups in aqueous solution. The co-staining of HeLa-S3 cells with **5** and LysoTracker disclosed that **5** is capable of staining lysosome, an acidic organelle in cells. Finally, the pH-dependent generation of $^1O_2$ and necrosis-like cell death of HeLa-S3 cells as the result of the photoirradiation of **5** are also reported.

EXPERIMENTAL SECTION

General Information. $IrCl_3·3H_2O$ and ethyl iodide were purchased from KANTO CHEMICAL Co. 1,3-Diphenylisobenzofuran (DPBF), carbonyl cyanide 3-chlorophenylhydrazone (CCCP), and concanamycin A was purchased from SIGMA-Aldrich. Propidium iodide (PI), 3-(4,5-dimethyl-2-thiazolyl)-2,5-diphenyl-2*H*-tetrazolium bromide (MTT), and organic solvent for spectroscopic analysis were purchased from WAKO CHEMICALS Co., Ltd. MEM (GIBCO Minimum Essential Medium), MitoTracker Red CMXRos, and LysoTracker Red DND-99 were purchased from Invitrogen. Annexin V-Cy3 was purchased from BioVision, Inc. All aqueous solutions were prepared using deionized water. $Ir(tpy)_3$ **2** and $Ir(atpy)_3$ **4** were prepared according to our previous paper.[26] Melting points were measured on a YANACO MP-33 Micro Melting Point Apparatus and are uncorrected. For measurement of UV−vis and luminescence spectra in aqueous solution at given pHs, buffer solutions (CHES, pH 10.0 and 9.0; EPPS, pH 8.0; HEPES, pH 7.4 and 7.0; MES, pH 6.5, 6.0, 5.0 and 4.0) were used. The Good's buffer reagents (Dojindo) were obtained from commercial sources: MES (2-morpholinoethanesulfonic acid, pK_a = 4.8), HEPES (2-[4-(2-hydroxyethyl)-1-piperazinyl]ethanesulfonic acid, pK_a = 7.5), EPPS (3-[4-(2-hydroxyethyl)-1-piperazinyl]propanesulfonic acid, pK_a = 8.0), CHES (2-(cyclohexylamino)ethanesulfonic acid, pK_a = 9.5). IR spectra were recorded on a Perkin-Elmer FTIR-Spectrum 100 (ATR). ^1H NMR (300 MHz) was recorded on a JEOL Always 300 spectrometer. Elemental analysis was performed on a Perkin-Elmer CHN 2400 analyzer. Thin-layer chromatography (TLC) was performed using TLC aluminum oxide 60 F_{254}, basic (Merck). Alumina column chromatography was performed using Merck aluminum oxide 90 active neutral. Luminescence imaging was performed using a fluorescence microscope (BIOREVO BZ-9000, Keyence). Confocal microscope imaging was performed using a confocal microscope (Leica TCS SP2, Leica). Emission lifetimes were determined using a TSP-1000 (Unisoku Co., Ltd.). Inductively coupled plasma atomic emission spectrometry (ICP−AES) measurements were performed on a Shimadzu ICPE-9000. Density functional theory (DFT) calculations were also carried out using the Gaussian03 program (B3LYP, the LanL2DZ basis set for a Ir atom, and the 6-31G basis set for H, C, N atoms).[27,29] The highest occupied molecular orbital (HOMO) and lowest unoccupied molecular orbital (LUMO) energies were obtained by single point calculation for the optimized structures of the Ir complexes.

***fac*-Tris[2-(5′-*N*,*N*-diethylamino-4′-tolyl)pyridine]iridium(III) (5).** A mixture of racemic **4** (149 mg, 0.216 mmol),[26] ethyl iodide (3.12 g, 20.0 mmol), and Cs_2CO_3 (652 mg, 2.00 mmol) in MeCN (7.20 mL) was stirred at room temperature for 16 h, and the insoluble materials were isolated on a filter and washed with $CHCl_3$. The filtrate was concentrated under the reduced pressure, and diluted with $CHCl_3$. The resulting $CHCl_3$ solution was washed with 2N NaOH aq. and the combined organic layer was dried over Na_2SO_4, filtered, and concentrated under the reduced pressure. The resulting residue was purified by alumina column chromatography ($CHCl_3$) and the eluted $CHCl_3$ solution containing **5** was washed with 2N NaOH aq. and concentrated (this manipulation is necessary to obtain clear ^1H NMR spectra). The resulting material was recrystallized from $CHCl_3$/hexane to afford **5** (as a racemic mixture) as a brown powder (36 mg, 20% from **4**). Mp >300 °C. IR (ATR): ν = 2966, 2926, 2868, 2809, 2023, 1692, 1600, 1467, 1427, 1373, 1256, 1227, 1156, 1123, 1066, 778, 748 cm^{-1}. ^1H NMR (300 MHz, DMSO-d_6/TMS): δ = 8.06 (d, J = 7.8 Hz, 3H), 7.72 (t, J = 7.8 Hz, 3H), 7.51 (m, 6H), 7.06 (t, J = 7.8 Hz, 3H), 6.30 (s, 3H), 2.89 (q, J = 6.9 Hz, 12H), 1.89 (s, 3H), 0,84 (t, J = 6.9 Hz, 18H) ppm. ESI-MS (m/z). Calcd for $C_{48}H_{59}IrN_6$ $(M+2H)^{2+}$: 455.2198, Found: 455.2192. Anal. Calcd for $C_{48}H_{57}IrN_6·0.5CHCl_3$: C, 60.06; H, 5.98; N, 8.66. Found: C, 60.25; H, 5.76; N, 8.47.

dx.doi.org/10.1021/ic301310q | *Inorg. Chem.* 2012, 51, 12697−12706

Measurements of UV−vis Absorption and Luminescence Spectra. UV/vis absorption spectra were recorded on a JASCO V-550 and V-630BIO UV−vis spectrophotometer and emission spectra were recorded on a JASCO FP-6200 spectrofluorometer, respectively, at 25.0 ± 0.1 °C. Solution samples were degassed for 10 min by Ar bubbling through the solution prior to the luminescence measurements. The quantum yields for luminescence (Φ) were determined by comparison with the integrated corrected emission spectrum of a quinine sulfate standard, whose emission quantum yield in 0.1 M H_2SO_4 was assumed to be 0.55 (excitation at 366 nm). The following equation was used to calculate emission quantum yields, in which Φ_s and Φ_r depict the quantum yields of the sample and reference compound, η_s and η_r are the refractive indexes of the solvents used for the measurements of the sample and reference, A_s and A_r are the absorbance of the sample and the reference, and I_s and I_r stand for the integrated areas under the emission spectra of the sample and reference, respectively (all Ir compounds for luminescence measurements were excited at 366 nm in this study). For the determination of Φ_s in mixed solvent systems, the η values of the main solvents were used for the calculation.

$$\Phi_s = \Phi_r(\eta_s^2 A_r I_s)/(\eta_r^2 A_s I_r)$$

Cell Culture and Luminescence Imaging. HeLa-S3 cells, which were provided by Dr. Tomoko Okada (National Institute of Advanced Industrial Science and Technology), were grown in MEM supplemented with 10% FCS (fetal calf serum) under 5% CO_2 at 37 °C. HeLa-S3 cells (2.0×10^5 cells/mL) were plated in 0.5 mL of MEM on 12 well plates (IWAKI) under the same conditions and allowed to adhere for 24 h. Subsequently, 0.5 mL of MEM containing **5** (20 μM) in MEM/DMSO (49/1) was added, and the samples in MEM/DMSO (99/1, v/v) were incubated at 37 °C under 5% CO_2 for 30 min. The culture medium was then removed and washed twice with PBS (phosphate buffered saline). Finally, 0.5 mL of MEM was added for luminescence imaging by fluorescence microscopy of the Ir complexes with excitation at 377 nm (FF01 filter (377 ± 50) nm was used for excitation to obtain emission images from Ir complexes). Co-staining with 10 μM **5** and 10 nM MitoTracker, and with 10 μM **5** and 100 nM LysoTracker was carried out with excitation at 540 nm for MitoTracker and LysoTracker.

Confocal Imaging. HeLa-S3 cells were grown on 12 mm microscope cover glasses that were put in a 24 well plate and pretreated with 0.01% poly-L-lysine solution in H_2O for 30 min. The sample preparation was similar to that of the luminescence imaging. After washing with PBS, the microscope cover glasses were mounted onto slides for measurements. Imaging was performed using a confocal microscope (Leica TCS SP2, Leica) with excitation wavelength at 350 and 360 nm for Ir complexes and 568 nm for MitoTracker and LysoTracker. The emission of Ir complexes was measured at 490−550 nm and that of MitoTracker and LysoTracker was measured at 590−620 nm by using a prism spectrometer.

Inductively Coupled Plasma−Atomic Emission Spectrometry (ICP−AES) experiments. HeLa-S3 cells were incubated in 100 mm-coating dishes under an atmosphere of 5% CO_2 at 37 °C for 72 h. The culture medium was removed, and the cells were washed gently with PBS (5 mL). The cell layer was then trypsinized under an atmosphere of 5% CO_2 at 37 °C. The numbers of HeLa-S3 cells were counted (ca. 1.3×10^6 cells), and these cells were incubated in MEM/DMSO (99/1, v/v) with **2** (10 μM), **4** (10 μM), and **5** (10 μM), respectively, under an atmosphere of 5% CO_2 at 37 °C for 30 min. The culture medium and trypsinized medium solution were transferred into 50 mL centrifuge tubes and centrifuged at 4 °C (1400 rpm for 7 min). The medium was removed and HeLa-S3 cells transferred to a 15 mL centrifuge tube with MEM (5 mL × 2). After centrifugation at 1400 rpm and 4 °C for 7 min, the medium solution was removed. After transferring the HeLa-S3 cells to a 1.5 mL eppendorf tube with MEM (0.45 mL × 2), they were centrifuged at 2000 rpm and 4 °C for 10 min, and the medium solution was removed. RIPA (Radio-Immunoprecipitation Assay) buffers (500 μL) were then added, and the sample was allowed to stand at 0 °C for 30 min. The solution was centrifuged at 15000 rpm and 4 °C for 10 min, and the supernatant liquid (400 μL) was diluted with 5% HCl aq. to give a final volume of 10 mL. The solution was centrifugated at 3000 rpm and 4 °C for 10 min for ICP-AES analysis on a Shimadzu ICPE-9000.

Singlet Oxygen Trapping Experiments in DMSO/H_2O (3/2). Solutions of Ir complexes (12 μM) in DMSO/H_2O (1.3/1.2, v/v) (2.5 mL) were aerated for 10 min, to which a solution of 300 μM 1,3-diphenylisobenzofuran (DPBF) in DMSO (500 μL) was added. The resulting solutions containing 10 μM Ir complex and 50 μM DPBF in DMSO/H_2O (3/2) were photoirradiated at 366 nm at 25 °C, and changes in the UV/vis spectra of DPBF were recorded.

Annexin V-Cy3 and PI Staining. HeLa-S3 cells were incubated in MEM/DMSO (99/1, v/v) containing Ir complexes (10 μM) for 30 min and etoposide (100 μM) for 6 h at 37 °C, and washed twice with PBS. After incubation with Annexin V-Cy3 for 10 min at room temperature and PI for 1 h at 37 °C,[30] respectively, the sample was washed twice with PBS. Similarly, Ir complexes were induced in HeLa-S3 cells under the same conditions, and successive photoirradiation at 377 nm was carried out for 1 h at 25 °C. Swollen membranes of cells were stained with Annexin V-Cy3 and PI under the same conditions, and washed twice with PBS. The treated HeLa-S3 cells were observed by BIOREVO BZ-9000 (excitation at 540 nm for Annexin V-Cy3 and PI).

RESULTS AND DISCUSSION

Design of Ir(deatpy)$_3$ 5. Prior to the design of the new Ir(III) complexes, we predicted the pK_a values of the tris(*N*,*N*-dialkylamino) derivatives of **2** based on the values for known aniline derivatives that contain *N*,*N*-dialkylamino groups. The pK_a values of *N*,*N*-dialkylanilines (**6a−e**, **7a-e**, and **8a-e**) (Chart 3) determined by potentiometric pH titrations and those cited

Chart 3

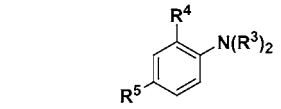

6a	R^3 = H	$R^4 = R^5$ = H
6b	R^3 = Me	
6c	R^3 = Et	
6d	R^3 = *n*-Pr	
6e	R^3 = *n*-Bu	
7a	R^3 = H	R^4 = Me, R^5 = H
7b	R^3 = Me	
7c	R^3 = Et	
7d	R^3 = *n*-Pr	
7e	R^3 = *n*-Bu	
8a	R^3 = H	R^4 = Me, R^5 = OMe
8b	R^3 = Me	
8c	R^3 = Et	
8d	R^3 = *n*-Pr	
8e	R^3 = *n*-Bu	

from the SciFinder database (numbers in parentheses) are summarized in Table S1 in the Supporting Information. The pK_a values of *N*,*N*-diethylaniline **6c** (R^3 = Et, $R^4 = R^5$ = H), *N*,*N*-diethyltoluidine **7c** (R^3 = Et, R^4 = Me, R^5 = H), and *N*,*N*-diethyl-4-methoxytoluidine **8c** (R^3 = Et, R^4 = Me, R^5 = OMe) were determined to be 6.5 ± 0.1, 7.2 ± 0.1, and 7.6 ± 0.1, respectively, by potentiometric pH titration, implying that the pK_a values of the diethylated aniline derivatives are about 2.0−2.9 (pK_a) units greater than those of the corresponding nonalkylated anilines, **6a**, **7a**, and **8a** (R^3 = H). From our previous work,[26] it was assumed that the C−Ir bonds in **2**, **4**, and **5** are electron donating, similar to a methoxy group. Thus, we chose the aniline derivatives having methyl and methoxy groups, **7a-e** and **8a-e** at the *para* position to the amino groups.

dx.doi.org/10.1021/ic301310q | Inorg. Chem. 2012, 51, 12697−12706

The numbers in parentheses are the estimated pK_a values cited from the SciFinder database, and are very close to those obtained by potentiometric pH titrations and reported previously. The pK_a values of *N,N*-dipropylanilines, **6d**, **7d**, **8d** (R^3 = *n*-Pr) and *N,N*-dibutylanilines, **6e**, **7e**, **8e** (R^3 = *n*-Bu) were only predicted by the database, because of their low solubility in aqueous solution. These results allowed us to predict that the pK_a of the tris(*N,N*-diethylamino) derivative of Ir(tpy)$_3$, at the ground state would be around 7.

Synthesis and Luminescence Emission Spectra of Ir(deatpy)$_3$ 5. On the basis of the aforementioned predictions, Ir(deatpy)$_3$ **5** was prepared as a racemic mixture (a mixture of Λ and Δ forms) from **4** with ethyl iodide and Cs_2CO_3 in 20% yield. Acid-free **5** exhibits an orange-colored emission at 554 nm in degassed DMSO, which is about 60 nm shorter than that of **4** (emission at 613 nm), as shown in Figure 1a.[31] The addition of H^+ to **5** induced a considerable enhancement in emission at 497 nm (green color emission), possibly because of the protonation of the three amino groups.

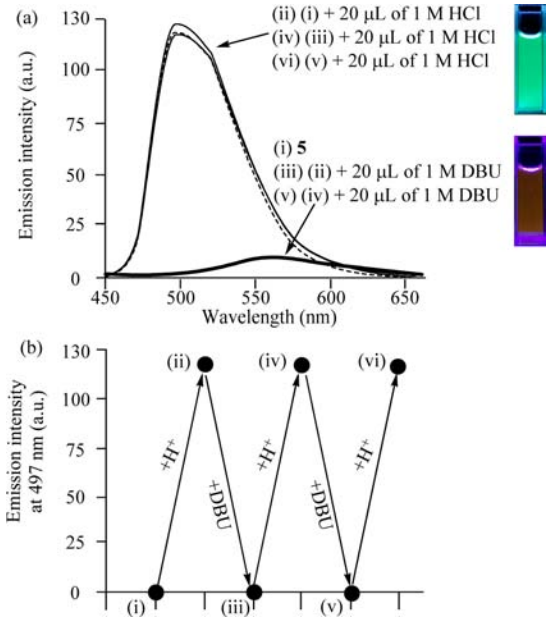

Figure 1. (a) Change in luminescence emission spectra of **5** (10 μM) in degassed DMSO at 25 °C (excitation at 366 nm) upon the repeated addition of acid (1 M HCl in 1,4-dioxane) and base (1 M DBU in 1,4-dioxane). (i) **5**, (ii) (i) + HCl, (iii) (ii) + DBU, (iv) (iii) + HCl, (v) (iv) + DBU, and (vi) (v) + HCl. A.u. is in arbitrary units. (b) Change in emission intensity of **5** at 497 nm caused by the repeated addition of HCl and DBU.

When DBU (1,8-diazabicyclo[5.4.0]undec-7-ene) was added as a base, the orange-colored emission was recovered and a reversible change in the emission intensity and wavelength were observed by repeated addition of acid and a base, as presented in Figure 1b. This reversibility of the protonated and acid-free species was also confirmed by ^{1}H NMR spectra measurement (Figure S3 in the Supporting Information).

Luminescence spectra of **5** (1 μM) in degassed DMSO/100 mM buffer (from pH 4 to 10) (1/4) at 298 K are shown in Figure 2a. Complex **5** exhibits a strong green emission (494 nm) at pH 4−6.5. The quantum yield (ϕ) and lifetime ($\tau^{1/2}$) of H_3·**5** in DMSO were determined to be 0.29 and 1.5 μs, respectively, which are not so different from the ϕ (0.23) and

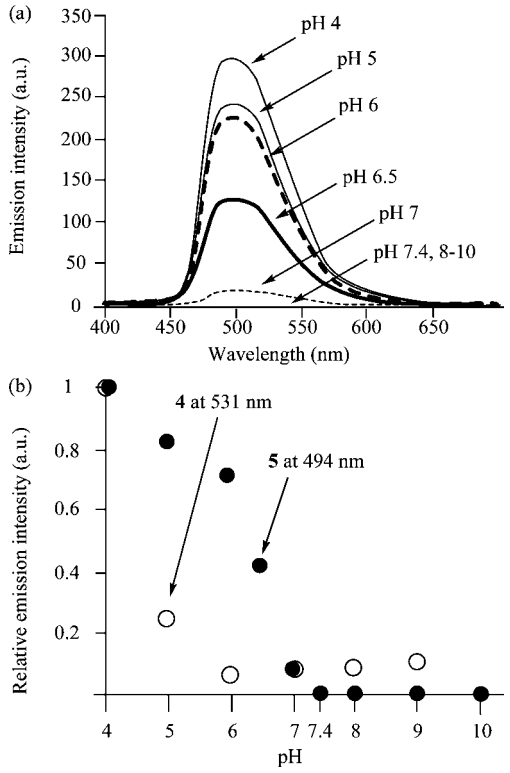

Figure 2. (a) Change in the emission spectra of **5** (1 μM) in degassed DMSO/100 mM buffer (from pH 4 to 10) (1/4) at 25 °C. (b) pH-Dependent emission intensity of **5** (1 μM) at 494 nm (closed circle) in degassed DMSO/100 mM Good's buffer (1/4) and that of **4** (100 μM) at 531 nm (open circle) in deggased DMSO/100 mM Good's buffer (1/6). This relative emission intensity of **4** and **5** was calculated based on 1 at pH 4. Excitation at 366 nm. A.u. is in arbitrary units.

$\tau^{1/2}$ (0.4 μs) values of H_3·**4** under the same conditions.[32,33] Very interestingly, the emission of **5** was very weak at pH >7. As shown in Figures 2b and 3, the threshold of emission intensity is shifted from pH 3−4 (for **4**)[26] to pH 7−7.4 (for **5**) when two ethyl groups are introduced to all three amino groups (Figure 2b), as predicted.

Both the pH-dependent change in UV/vis absorbance at 277 nm (Figure S2 in the Supporting Information) and the emission intensity at 494 nm of **5** (Figure 2) suggests that the pK_a values of **5** in the ground state and excited state are nearly identical (Figure S6a in the Supporting Information). Similar phenomena were observed in the case of Ir(atpy)$_3$ **4** in our previous study.[26] More careful emission titration of **5** was performed from pH 8 to pH 4 (pH of a solution of **5** in DMSO/100 μM MES buffer was changed from pH 8 to 4 by addition of 10 mM HCl aq. and emission spectra of the solution were measured at each step), and its result is shown in Figure S6b in the Supporting Information. On the basis of Figure S2 (inset) and S6b, it is likely that the first and second protonation occurs at pH 5−7 and the third protonation proceeds at pH <5, the values that are somewhat lower than the expected pK_a value.

Figure 4 shows the emission spectra of **5** in the presence of 1, 2, and 3 equiv of HCl in DMSO. The luminescence emission exhibited a blue-shift from 554 to 493 nm upon the addition of 1 equiv of H^+, and a second and third protonation induced an enhancement in the emission intensity at almost the same wavelength, suggesting that the blue-shift in the emission of **5** is induced by monoprotonation and the second and third

dx.doi.org/10.1021/ic301310q | *Inorg. Chem.* 2012, 51, 12697−12706

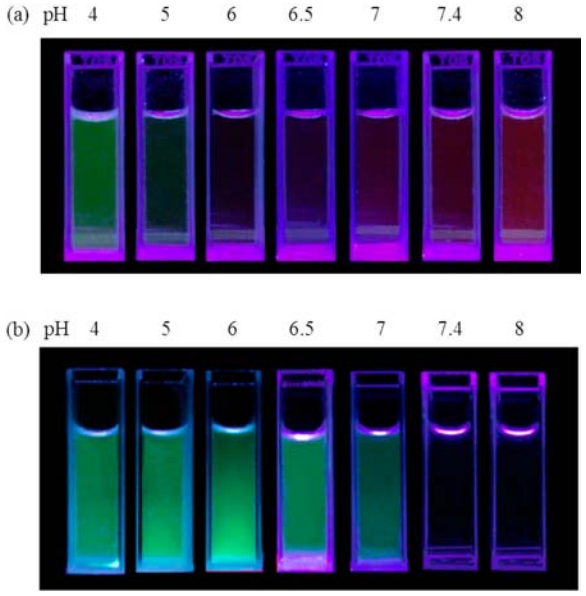

Figure 3. Photograph showing solutions of (a) **4** (100 μM) and (b) **5** (1 μM) in degassed DMSO/100 mM buffer (from pH 4 to 8) at 25 °C. Excitation at 365 nm.

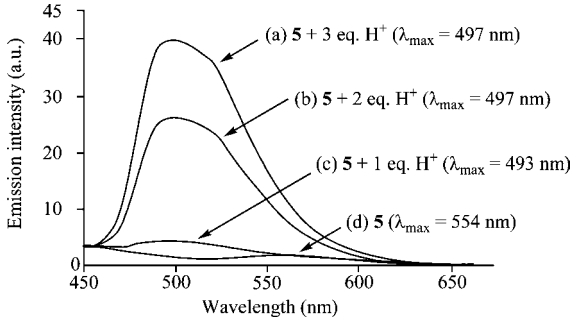

Figure 4. Emission spectra of **5** (100 μM) in DMSO in the presence of (a) 300 μM HCl, (b) 200 μM HCl, (c) 100 μM HCl and (d) 0 μM HCl at 25 °C. Excitation at 366 nm. A.u. is in arbitrary units.

protonation contribute to the enhancement in luminescence at about 500 nm. These results indicate Ir complex **5** is a useful on−off pH probe. It is known that emission of Ir complex is quenched by molecular oxygen, resulting in the generation of $^1O_2$.[20a,24e] The same phenomena were observed for H_3·**5** (Figure S7 in the Supporting Information).

Density functional theory (DFT) calculations were carried out for **2**, **4**, H_3·**4**, **5**, and H_3·**5** using the Gaussian03 program (B3LYP, LanL2DZ basis set for an Ir atom and the 6-31G basis set for H, C, N atoms). The HOMO and LUMO energies were obtained by single point calculation of the optimized Ir complexes. As shown in Figure S8 in the Supporting Information, the protonation of three amino groups of **4** and **5** induces the increase in HOMO−LUMO gap, supporting the considerable blue shift of emission wavelength of these Ir complexes. Time-dependent DFT (TD-DFT) calculations also support the intraligand charge transfer (^{3}ILCT) character from amino group to tpy ligand of **5**, and a thermally accessible ^{3}ILCT state may explain the low quantum yield of acid-free **5**. The triprotonated form does not exhibit the ^{3}ILCT state anymore, resulting in strong emission from ^{3}MLCT and ^{3}LC state.[8m,34]

Live Cell Imaging Using 5 with MitoTracker and LysoTracker. The aforementioned photochemical properties of **5** prompted us to use it in the staining of living cells. After incubation HeLa-S3 cells in MEM/DMSO (pH 7.4, 99/1, v/v) with **2**, **4**, and **5** (10 μM) for 30 min at 37 °C and washing with PBS, the cells were observed by a fluorescent microscopy (BIOREVO BZ-9000, Keyence).[35] It was of interest that clear luminescent images were obtained in the presence of **2** and **5** (Figure 5b and 5h). The emission of **2** is delocalized in the

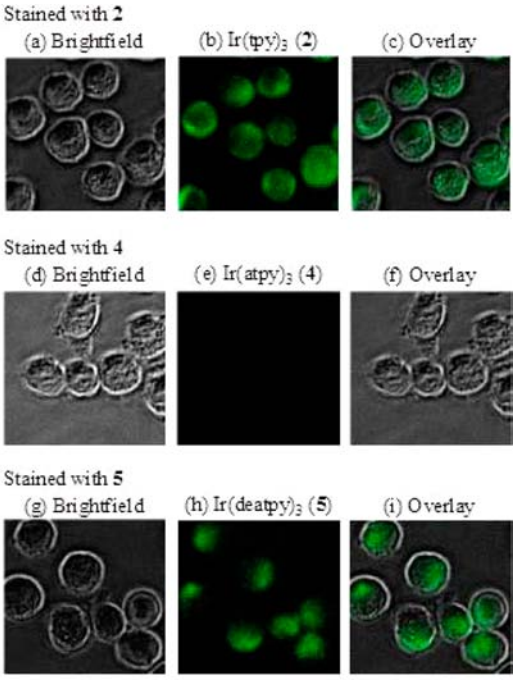

Figure 5. Luminescence microscopic images (×40) (BIOREVO BZ-9000, Keyence, excitation at 377 nm) of HeLa-S3 cells after incubation with **2** (10 μM), **4** (10 μM), and **5** (10 μM) in MEM/DMSO (99/1, v/v) at 37 °C for 30 min respectively. (a) Brightfield image of HeLa-S3 with **2**, (b) emission image with **2**, (c) overlay image of (a) + (b), (d) brightfield image with **4**, (e) emission image with **4**, (f) overlay image of (d) + (e), (g) brightfield image with **5**, (h) emission image with **5**, (i) overlay image of (g) + (h).

cytosol of HeLa-S3 cells (Figure 5b and 5c), rather than nuclei. For comparison, Figure 5d−f showed negligible emission from **4**. On the other hand, the luminescence image of **5** exhibits a strong emission at a specific area in cells, as shown in Figure 5h and 5i. Moreover, luminescence microscopic observations of HeLa-S3 cells with on−off probe **5** does not require washing with PBS buffer, while **2** emits in both cells and the background solution under the same conditions (Figure S11 in the Supporting Information).

The intracellular concentrations of **2**, **4**, and **5** in HeLa-S3 cells were investigated by ICP-AES measurements. As summarized in Table 1, the concentration of the cellular uptake of **2**, **4**, and **5** were determined to be 0.27, 0.25, and 0.20 fmol/cell, respectively, indicating these three Ir complexes are transferred into cells at nearly the same extent. It should be noted that the almost same cellular uptake phenomena of **2**, **4**, and **5** were also observed at 4 °C (Figure S12 in the Supporting Information),[15,17,18b] suggesting that these complexes were taken up by living cells by passive transport.

It is reported that CCCP (carbonyl cyanide 3-chlorophenylhydrazone) inhibits oxidative phosphorylation, decreases

dx.doi.org/10.1021/ic301310q | Inorg. Chem. 2012, 51, 12697−12706

Table 1. Amount of Ir Complexes (2, 4, and 5) in HeLa-S3 Cells Determined by ICP-AES Measurement after Incubation with 2 (10 μM), 4 (10 μM), and 5 (10 μM) at 37 °C for 30 min

complex	mols per cell (fmol/cell)
2 ($Ir(tpy)_3$)	0.27
4 ($Ir(atpy)_3$)	0.25
5 ($Ir(deatpy)_3$)	0.20

ATP production, and lowers metabolic rate, resulting in the suppression of active transport. For instance, Lo and co-workers explained cellular uptake mechanism of bis-cyclometalated Ir(III) complexes by using CCCP.[13c] Incubation of HeLa-S3 cells with CCCP (20 μM) at 37 °C for 30 min in MEM/DMSO (990/5) and then staining with **2** (10 μM) and **5** (10 μM) gave similar emission images (Figure S13 in the Supporting Information) as those in Figure 5. These results together with aforementioned results of the cellular uptake at 4 °C support passive transport of **2** and **5** into the cells. Careful observation of HeLa-S3 cells treated with CCCP and then **5** suggests that emission of **5** is distributed not only to lysosome, but also other organelles, possibly because pH values of some organelles are compromised by CCCP.[36,37]

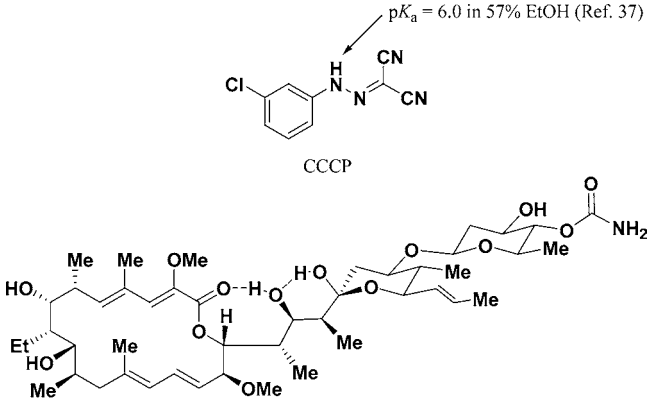

In the next experiments, co-staining studies of **2** or **5** with a lysosomal dye (LysoTracker) and a mitochondrial dye (MitoTracker) were conducted, because it is known that the pH of lysosomes is lower than 5.5[1] and the pH of mitochondria is about 7.5.[2] Figure 6a–d display a typical brightfield image (Figure 6a), a luminescent image of **2** (Figure 6b), a luminescent image of MitoTracker (Figure 6c), and a merged image of Figure 6b and 6c (Figure 6d). It is likely that the area stained by **2** and MitoTracker are largely overlapped. Figure 6e–h show the results for the co-staining of HeLa-S3 cells with **2** and LysoTracker. Merged images of Figures 6d and 6h show wide yellow regions, indicating that **2** is delocalized in mitochondria and lysosomes as well as the cytosol.

The typical brightfield image, luminescent image with **5** and MitoTracker and their merged image (Figure 6i–l) indicate that **5** is negligibly overlapped with MitoTracker. On the other hand, the luminescent overlay image (Figure 6p) of **5** (Figure 6n) and LysoTracker (Figure 6o) clearly shows some yellow regions, indicating that **5** and LysoTracker stained the same organelles.[38,39] These results suggest that acid-free **5** exhibits negligible emission in neutral~basic organelles such as mitochondria, and the protonation of diethylamino groups of **5** induces a strong green emission in acidic organelles such as lysosomes. These results are consistent with the luminescent

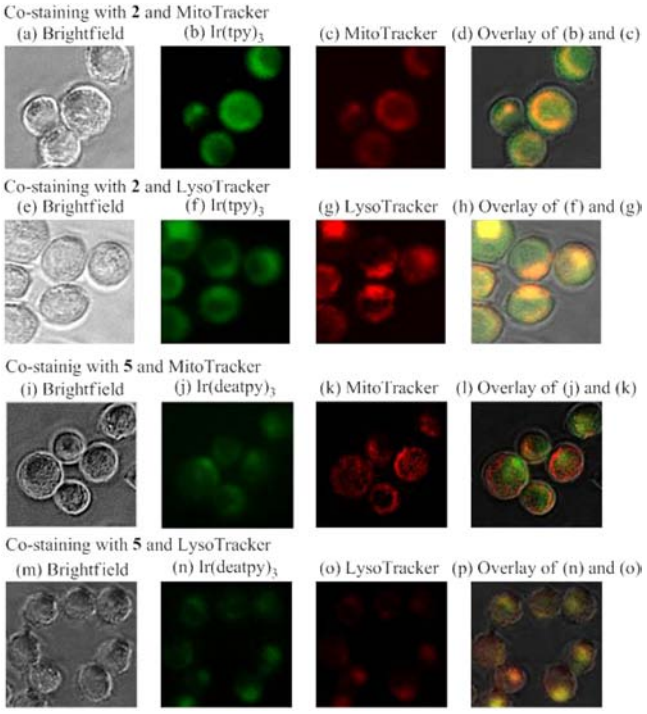

Figure 6. Luminescence microscope images (BIOREVO BZ-9000, Keyence) of HeLa-S3 cells (× 40) stained with Ir complexes (10 μM), MitoTracker (10 nM), or LysoTracker (100 nM) in MEM/DMSO (99/1, v/v) at 37 °C for 30 min. (a), (e), (i), and (m) brightfield images of HeLa-S3, (b) and (f) emission images of **2**, (j) and (n) emission images of **5**, (c) and (k) emission images of MitoTracker, (g) and (o) emission images of LysoTracker, (d) overlay image of (a), (b) and (c), (h) overlay image of (e), (f), and (g), (l) overlay image (i), (j), and (k), (p) overlay image (m), (n), and (o). Excitation at 377 nm for Ir complexes and excitation at 540 nm for MitoTracker and LysoTracker.

behaviors of **5** in the aqueous solution shown in Figures 2 and 3.

It is reported that concanamycin A inhibits V-ATPase, and decreases proton transfer in organelles such as endosomes and lysosomes, resulting in the suppression acidification of organelles.[40,41] Incubation of HeLa-S3 cells with concanamycin A (500 nM) at 37 °C for 60 min in MEM/DMSO (990/5), before incubation with **5** (10 μM) and LysoTracker (100 nM), led to a considerable decrease of emission intensity (Figure S15 in the Supporting Information). These data support emission of **5** is considerably enhanced in acidic organelles.

Generation of Singlet Oxygen by the Photoirradiation of Ir Complexes. The generation of singlet oxygen ($^1O_2$)[42] by Ir complexes or methylene blue (10 μM) in DMSO/H_2O (3/2) upon photoirradiation at 366 nm for Ir complexes and 575 nm for methylene blue was measured by change in UV/vis spectra of 1,3-diphenylisobenzofuran (DPBF),[23c,25c,43] whose absorbance at 415 nm decreases by the reaction with $^1O_2$. In Figure 7, $^1O_2$ generation of Ir complexes were compared with that of methylene blue, which is a well-known pH sensitive photosensitizer and induces apoptosis-like cell death via a mitochondria-dependent pathway.[23e,25a] Generation of $^1O_2$ by photoirradiated **2** (Figure 7c) was similar to that of methylene blue (Figure 7d). On the other hand, it was found that generation of $^1O_2$ by **4**, H_3·**4**, and **5** were equal to that of blank (Figure 7a). Interestingly, $^1O_2$ generation activity of **5** is restored by protonation of the

dx.doi.org/10.1021/ic301310q | Inorg. Chem. 2012, 51, 12697–12706

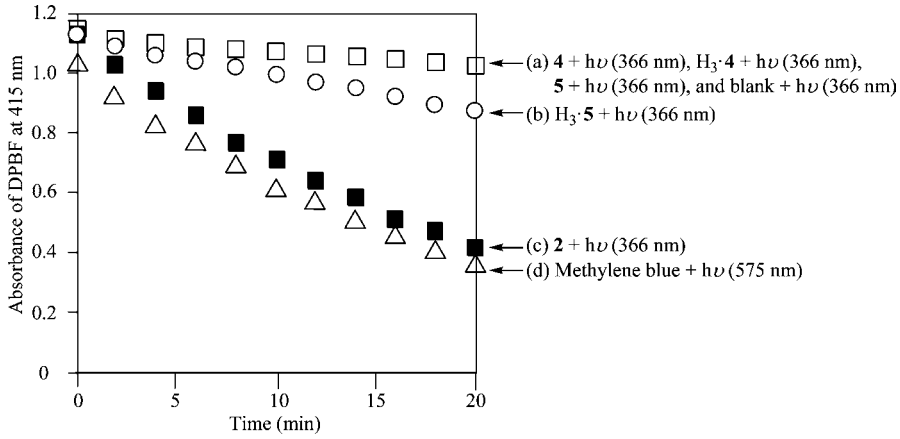

Figure 7. Comparative photooxidation of 1,3-diphenylisobenzofuran (DPBF) (50 μM) in DMSO/H_2O (3/2), (a) **4**, H_3·**4**, **5** (10 μM), and blank in DMSO/H_2O (3/2) (open squares), (b) **5** (10 μM) and HCl (50 μM) in DMSO/H_2O (3/2) (open circles), (c) **2** (10 μM) in DMSO/H_2O (3/2) (closed squares), (d) methylene blue (10 μM) in DMSO/H_2O (3/2) (open triangles). Excitation at 366 nm (Ir complexes) and 575 nm (methylene blue), at which absorbance of methylene blue (at 575 nm) and **5** at (366 nm) are almost identical at 10 μM.

diethylamino groups (Figure 7b). This property is similar to that of O'shea's BF_2-chelated azadipyrromethene derivative,[25c] and is opposite to the characteristics of methylene blue.[25a] DPBF was negligibly decomposed without photoirradiation even in the presence of **2** (data not shown). In addition, its decomposition was suppressed in the presence of **2** (10 μM) with photoirradiation in degassed by Ar (Figure S16 in the Supporting Information). These results strongly suggest negligible direct photoreaction between Ir complexes and DPBF.

Induction of Cell Death of HeLa-S3 Cells upon Photoirradiation in the Presence of Ir Complexes. We were interested in whether photoirradiation of **5** would be able to generate $^1O_2$ enough to induce cell death under the intracellular environment, in which clear emission is observed from **5**, possibly because of rather low O_2 concentration. Figure 8 shows timelapse images of HeLa-S3 cells with **5** (10 μM) and

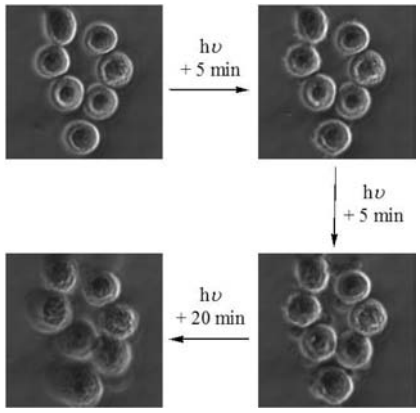

Figure 8. Luminescence microscope images (BIOREVO BZ-9000, Keyence) showing membrane swelling of HeLa-S3 cells (× 40) upon photoirradiation at 377 nm in the presence of **5** (10 μM).

photoirradiation at 377 nm for 30 min. After photoirradiation for 5 min, the membranes of HeLa-S3 cells began to swell and this swelling continued during the period of photoirradiation. The same phenomena were also observed in the case of **2** under the same conditions. In addition, similar results were obtained by photoirradiation at 470 nm, which would be expected to exhibit lower damage to living cells (Table S3 in the Supporting Information). On the other hand, negligible membrane swelling was observed by photoirradiation without **5** or no photoirradiation in the presence of **5**. These results indicate that the swelling of the cell membrane was caused by the photoirradiation of Ir complexes **2** and **5**.[44] Interestingly, the swelling of cell membranes by **4** was negligible when the sample was subjected to photoirradiation at 377 nm for 60 min (Table S3 in the Supporting Information). Consideration of these phenomena, together with the results of the photochemical generation of $^1O_2$ by **2**, **4**, and **5** shown in Figure 7, indicate that the cell death of HeLa-S3 cells is caused by $^1O_2$.

We asked ourselves whether this photoinduced cell death of HeLa-S3 cells is apoptosis or necrosis (or necrosis-like[45])? To answer this question, we performed co-staining of HeLa-S3 with **5** and Annexin V-Cy3 (Figure 9),[30] since Annexin V binds to negatively charged phosphatidyl serine residues on the membranes of apoptotic cells as well as necrotic cells, and fluorescein isothiocynate (Cy-3)-labeled annexin V is a good indicator of apoptotic and necrotic cells. On the other hand, propidium iodide (PI) stains necrotic cells rather than apoptotic cells.

Figure 9a–c show a brightfield image (Figure 9a), Annexin V-Cy3 emission image (Figure 9b), and a PI emission image (Figure 9c) in the presence of **2** without photoirradiation, showing a negligible red emission of Annexin V-Cy3 and PI. Figure 9d–f displays a brightfield image, an Annexin V-Cy3 emission image, and a PI emission image after photoirradiation at 377 nm in the presence of **2** (10 μM). Cell membrane swelling was observed in Figure 9d and Annexin V-Cy3 emission on the cell membrane (Figure 9e) and PI emission in the cells (Figure 9f) were observed. Similar images were observed in the case of **5** under the same conditions (Figure 9g–i). Furthermore, these images were compared with cell death induced by etoposide, which is an inducer of apoptosis in cancer cells. Indeed, Annexin V-Cy3 emission was observed in Figure 9k and PI emission was negligible in Figure 9l. These experimental data suggest that the photoirradiation of Ir complexes **2** or **5** mainly induces necrosis-like cell death in HeLa-S3 cells. The difference of mechanisms in a cell death of HeLa-S3 cells treated with **5** + photoirradiation and those treated with etoposide is supported by comparison of these morphological features. Figure 10 shows results of cell viability

dx.doi.org/10.1021/ic301310q | Inorg. Chem. 2012, 51, 12697–12706

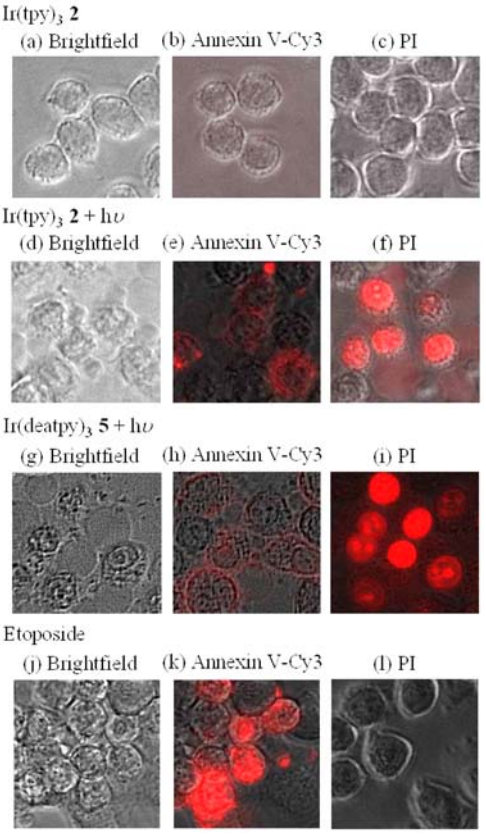

Figure 9. Fluorescence microscope images (BIOREVO BZ-9000, Keyence) of HeLa-S3 cells (×40) irradiated at 377 nm (except (a), (b), (c), (j), (k), and (l)) for 1 h after preincubation with **2** (10 μM), **5** (10 μM), and etoposide (100 μM), and stained with Annexin V-Cy3, and PI (30 μM). Excitation at 540 nm to observe Annexin V-Cy3 and PI. (a), (d), (g), and (j) brightfield images of HeLa-S3, (b), (e), (h), and (k) emission images of Annexin V-Cy3, (c), (f), (i), and (l) emission images of PI.

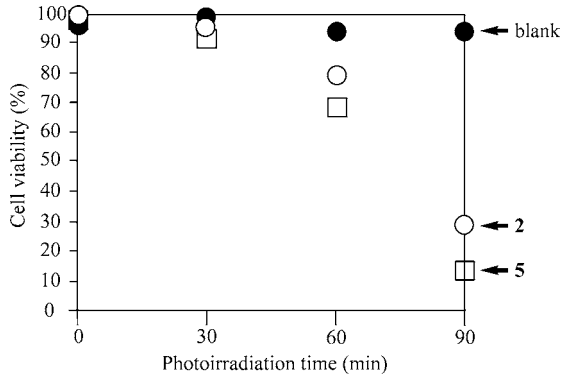

Figure 10. Change in cell viability of HeLa-S3 cells monitored by PI-staining upon photoirradiation at 377 nm in the absence (closed circles), and presence of **2** (10 μM) (open circles) and (c) **5** (10 μM) (open squares) in MEM/DMSO (99/1). Cell viability (%) = (number of cells which were not stained by PI/number of all cells) × 100.

of HeLa-S3 cells after photoirradiation at 377 nm in the absence (closed circles) and in the presence of **2** (10 μM) (open circles) and **5** (10 μM) (open squares) by PI staining. These results afforded further evidence for the necrosis-like cell death promoted by photoactivation of Ir complexes.

It has been reported that massive lysosomal breakdown by reactive oxygen species such as $^1O_2$ induces cellular necrosis-like cell death, while a partial and selective lysosomal breakdown is associated with induction of apoptosis.[46] Consideration of this collective information, together with our results showing that **5** is possibly protonated in lysosomes and the protonated forms of **5** generate $^1O_2$ more effectively than acid-free **5**, may explain the photoinduced necrosis-like cell death of HeLa-S3 cells.

■ CONCLUSIONS

In summary, we report on the synthesis, characterization, photochemical properties, cellular imaging, and photosensitizer activity of a new pH-sensitive Ir(III) complex **5** that contains three *N*,*N*-diethylamino groups, whose pK_a value was predicted from the pK_a values of some known *N*,*N*-dialkyl aniline derivatives. The luminescence emission of **5** in DMSO was found to be orange colored at 554 nm, and was at a wavelength about 60 nm shorter than that of **4**. The addition of H^+ to **5** induced a considerable enhancement in green color at 497 nm because of the protonation of the three amino groups. In aqueous solutions, the emission intensity of **5** at 494 nm is very weak at pH >7.4 and is considerably enhanced at pH <7. A cellular imaging study of HeLa-S3 cells with **5**, LysoTracker, and MitoTracker provides effective evidence that emission of **5** is considerably enhanced in lysosomes. Photoirradiation of **5** induces the generation of $^1O_2$ under acidic conditions rather than basic conditions. The photoirradiation of **2** or **5** induces the cell death of HeLa-S3 cells, mainly via necrosis-like cell death. It is intriguing that, to the best of our knowledge, complex **5** is a first example of a cyclometalated Ir(III) complex that functions as a phosphorescent on−off pH-probe and a pH-dependent $^1O_2$ generator for inducing necrosis-like cell death. Our results provide a useful strategy for the future design and synthesis of phosphorescent on−off pH probe based on Ir complex and biologically active compounds for the diagnosis and treatment of various types of cancer and related diseases.[47,48]

■ ASSOCIATED CONTENT

Ⓢ Supporting Information

Figures S1−S16 and Tables S1−S3. This material is available free of charge via the Internet at http://pubs.acs.org.

■ AUTHOR INFORMATION

Corresponding Author

*E-mail: shinaoki@rs.noda.tus.ac.jp.

Notes

The authors declare no competing financial interest.

■ ACKNOWLEDGMENTS

This study was supported by Grants-in-Aid from the Ministry of Education, Culture, Sports, Science and Technology (MEXT) of Japan (No. 22890200 for Y.H. and No. 19659026, 22390005, 22659005, and 24659058 for S.A.) and "Academic Frontier" project for private universities: matching fund subsidy from MEXT, 2009−2013. We appreciate Prof. Makoto Yuasa, Mr. Tomohide Saito, Ms. Takako Yamaguchi, Mr. Yoshitaka Katsuta (Faculty of Science and Technology, Tokyo University of Science), and Prof. Masahiro Kohno (Tokyo Institute of Technology) for helpful discussion.

REFERENCES

(1) Demaurex, N. *News Physiol. Sci.* **2002**, *17*, 1−5.
(2) Orij, R.; Postmus, J.; Beek, A. T.; Brul, S.; Smits, G. J. *Microbiology* **2009**, *155*, 268−278.
(3) Volk, T.; Jähde, E.; Fortmeyer, H. P.; Glüsenkamp, K.-H.; Rajewsky, M. F. *Br. J. Cancer* **1993**, *68*, 492−500.
(4) Han, J.; Burgess, K. *Chem. Rev.* **2010**, *110*, 2709−2728.
(5) For example of lysosome selective fluorescent probes: (a) Glunde, K.; Foss, C. A.; Takagi, T.; Wildes, F.; Bhujwalla, Z. M. *Bioconjugate Chem.* **2005**, *16*, 843−851. (b) Freundt, E. C.; Czapiga, M.; Lenardo, M. J. *Cell Res.* **2007**, *17*, 956−958. (c) Gao, Y.; Wu, J.; Li, Y.; Sun, P.; Zhou, H.; Yang, J.; Zhang, S.; Jin, B.; Tian, Y. *J. Am. Chem. Soc.* **2009**, *131*, 5208−5213. (d) Wang, X.; Nguyen, D. M.; Yanez, C. O.; Rodriguez, L.; Ahn, H.-Y.; Bondar, M. V.; Belfield, K. D. *J. Am. Chem. Soc.* **2010**, *132*, 12237−12239. (e) Fan, F.; Nie, S.; Yang, D.; Luo, M.; Shi, H.; Zhang, Y.-H. *Bioconjugate Chem.* **2012**, *23*, 1309−1317.
(6) (a) Urano, Y.; Asanuma, D.; Hama, Y.; Koyama, Y.; Barrett, T.; Kamiya, M.; Nagano, T.; Watanabe, T.; Hasegawa, A.; Choyke, P. L.; Kobayashi, H. *Nat. Med.* **2009**, *15*, 104−109. (b) Hoogendoorn, S.; Habets, K. L.; Passemard, S.; Kuiper, J.; van der Marel, G. A.; Florea, B. I.; Overkleeft, H. S. *Chem. Commun.* **2011**, *47*, 9363−9365.
(7) Berezin, M. Y.; Achilefu, S. *Chem. Rev.* **2010**, *110*, 2641−2684.
(8) (a) Lamansky, S.; Djurovich, P.; Murphy, D.; Abdel-Razzaq, F.; Kwong, R.; Tsyba, I.; Bortz, M.; Mui, B.; Bau, R.; Thompson, M. E. *Inorg. Chem.* **2001**, *40*, 1704−1711. (b) Tamayo, A. B.; Alleyne, B. D.; Djurovich, P. I.; Lamansky, S.; Tsyba, I.; Ho, N. N.; Bau, R.; Thompson, M. E. *J. Am. Chem. Soc.* **2003**, *125*, 7377−7387. (c) Lowry, M. S.; Bernhard, S. *Chem.—Eur. J.* **2006**, *12*, 7970−7977. (d) Obara, S.; Itabashi, M.; Okuda, F.; Tamaki, S.; Tanabe, Y.; Ishii, Y.; Nozaki, K.; Haga, M. *Inorg. Chem.* **2006**, *45*, 8907−8921. (e) Flamigni, L.; Barbieri, A.; Sabatini, C.; Ventura, B.; Barigelletti, F. *Top. Curr. Chem.* **2007**, *281*, 143−203. (f) Ulbricht, C.; Beyer, B.; Friebe, C.; Winter, A.; Schubert, U. S. *Adv. Mater.* **2009**, *21*, 4418−4441. (g) You, Y.; Park, S. Y. *Dalton Trans.* **2009**, 1267−1282. (h) Kim, E.; Park, S. B. *Chem.—Asian J.* **2009**, *4*, 1646−1658. (i) Wong, W.-Y.; Ho, C.-L. *Coord. Chem. Rev.* **2009**, *253*, 1709−1758. (j) Chi, Y.; Chou, P.-T. *Chem. Soc. Rev.* **2010**, *39*, 638−655. (k) Ladouceur, S.; Fortin, D.; Zysman-Colman, E. *Inorg. Chem.* **2011**, *50*, 11514−11526. (l) Ito, A.; Hiokawa, T.; Sakuda, E.; Kitamura, N. *Chem. Lett.* **2011**, *40*, 34−36. (m) You, Y.; Nam, W. *Chem. Soc. Rev.* **2012**, *41*, 7061−7084.
(9) (a) Baldo, M. A.; O'Brien, D. F.; You, Y.; Shoustikov, A.; Sibley, S.; Thompson, M. E.; Forrest, S. R. *Nature* **1998**, *395*, 151−154. (b) Tsuboyama, A.; Iwawaki, H.; Furugori, M.; Mukaide, T.; Kamatani, J.; Igawa, S.; Moriyama, T.; Miura, S.; Takiguchi, T.; Okada, S.; Hoshino, M.; Ueno, K. *J. Am. Chem. Soc.* **2003**, *125*, 12971−12979. (c) Ren, X.; Alleyne, B. D.; Djurovich, P. I.; Adachi, C.; Tsyba, I.; Bau, R.; Thompson, M. E. *Inorg. Chem.* **2004**, *43*, 1697−1707. (d) Hwang, F.-M.; Chen, H.-Y.; Chen, P.-S.; Liu, C.-S.; Chi, Y.; Shu, C.-F.; Wu, F.-I.; Chou, P.-T.; Peng, S.-M.; Lee, G.-H. *Inorg. Chem.* **2005**, *44*, 1344−1353. (e) Okada, S.; Okinaka, K.; Iwawaki, H.; Furugori, M.; Hashimoto, M.; Mukaide, T.; Kamatani, J.; Igawa, S.; Tsuboyama, A.; Takiguchi, T.; Ueno, K. *Dalton Trans.* **2005**, 1583−1590. (f) Evans, R. C.; Douglas, P.; Winscom, C. J. *Coord. Chem. Rev.* **2006**, *250*, 2093−2126. (g) Song, Y.-H.; Chiu, Y.-C.; Chi, Y.; Cheng, Y.-M.; Lai, C.-H.; Chou, P.-T.; Wong, K.-T.; Tsai, M.-H.; Wu, C.-C. *Chem.—Eur. J.* **2008**, *14*, 5423−5434. (h) Farinola, G. M.; Ragni, R. *Chem. Soc. Rev.* **2011**, *40*, 3467−3482.
(10) (a) Marco, G. D.; Lanza, M.; Mamo, A.; Stefio, I.; Pietro, C. D.; Romeo, G.; Campagna, S. *Anal. Chem.* **1998**, *70*, 5019−5023. (b) DeRosa, M. C.; Mosher, P. J.; Yap, G. P. A.; Focsaneanu, K.-S.; Crutchley, R. J.; Evans, C. E. B. *Inorg. Chem.* **2003**, *42*, 4864−4872.
(11) (a) Licini, M.; Williams, J. A. G. *Chem. Commun.* **1999**, 1943−1944. (b) Arm, K. J.; Leslie, W.; Williams, J. A. G. *Inorg. Chim. Acta* **2006**, *359*, 1222−1232. (c) Ho, M.-L.; Hwang, F.-M.; Chen, P.-N.; Hu, Y.-H.; Cheng, Y.-M.; Chen, K.-S.; Lee, G.-H.; Chi, Y.; Chou, P.-T. *Org. Biomol. Chem.* **2006**, *4*, 98−103. (d) Konishi, K.; Yamaguchi, H.; Harada, A. *Chem. Lett.* **2006**, *35*, 720−721. (e) Schmittel, M.; Lin, H. *Inorg. Chem.* **2007**, *46*, 9139−9145. (f) Zhao, Q.; Cao, T.; Li, F.; Li, X.; Jing, H.; Yi, T.; Huang, C. *Organometallics* **2007**, *26*, 2077−2081. (g) Zhao, N.; Wu, Y.-H.; Wen, H.-M.; Zhang, X.; Chen, Z.-N. *Organometallics* **2009**, *28*, 5603−5611. (h) Brandel, J.; Sairenji, M.; Ichikawa, K.; Nabeshima, T. *Chem. Commun.* **2010**, *46*, 3958−3960. (i) Zhao, Q.; Li, F.; Huang, C. *Chem. Soc. Rev.* **2010**, *39*, 3007−3030.
(12) (a) Lo, K. K.-W.; Louie, M.-W.; Zhang, K. Y. *Coord. Chem. Rev.* **2010**, *254*, 2603−2622. (b) Lo, K. K.-W.; Li, S. P.-Y.; Zhang, K. Y. *New J. Chem.* **2011**, *35*, 265−287. (c) Zhao, Q.; Huang, C.; Li, F. *Chem. Soc. Rev.* **2011**, *40*, 2508−2524.
(13) (a) Kwon, T.-H.; Kwon, J.; Hong, J.-I. *J. Am. Chem. Soc.* **2008**, *130*, 3726−3727. (b) Lo, K. K.-W.; Zhang, K. Y.; Leung, S.-K.; Tang, M.-C. *Angew. Chem., Int. Ed.* **2008**, *47*, 2213−2216. (c) Lau, J. S.-Y.; Lee, P.-K.; Tsang, K. H.-K.; Ng, C. H.-C.; Lam, Y.-W.; Cheng, S.-H.; Lo, K. K.-W. *Inorg. Chem.* **2009**, *48*, 708−718. (d) Zhang, K. Y.; Lo, K. K.-W. *Inorg. Chem.* **2009**, *48*, 6011−6025. (e) Leung, S.-K.; Kwok, K. Y.; Zhang, K. Y.; Lo, K. K.-W. *Inorg. Chem.* **2010**, *49*, 4984−4995.
(14) (a) Zhang, K. Y.; Li, S. P.-Y.; Zhu, N.; Or, I. W.-S.; Cheung, M. S.-H.; Lam, Y.-W.; Lo, K. K.-W. *Inorg. Chem.* **2010**, *49*, 2530−2540. (b) Zhang, K. Y.; Liu, H.-W.; Fong, T. T.-H.; Chen, X.-G.; Lo, K. K.-W. *Inorg. Chem.* **2010**, *49*, 5432−5443.
(15) Li, C.; Yu, M.; Sun, Y.; Wu, Y.; Huang, C.; Li, F. *J. Am. Chem. Soc.* **2011**, *133*, 11231−11239.
(16) (a) Lo, K. K.-W.; Lee, P.-K.; Lau, J. S.-Y. *Organometallics* **2008**, *27*, 2998−3006. (b) Zhao, Q.; Yu, M.; Shi, L.; Liu, S.; Li, C.; Shi, M.; Zhou, Z.; Huang, C.; Li, F. *Organometallics* **2010**, *29*, 1085−1091. (c) Wu, H.; Yang, T.; Zhao, Q.; Zhou, J.; Li, C.; Li, F. *Dalton Trans.* **2011**, *40*, 1969−1976.
(17) Lee, P.-K.; Liu, H.-W.; Yiu, S.-M.; Louie, M.-W.; Lo, K. K.-W. *Dalton Trans.* **2011**, *40*, 2180−2189.
(18) (a) Murphy, L.; Congreve, A.; Pålsson, L.-O.; Williams, J. A. G. *Chem. Commun.* **2010**, *46*, 8743−8745. (b) Steunenberg, P.; Ruggi, A.; van den Berg, N. S.; Buckle, T.; Kuil, J.; van Leeuwen, F. W. B.; Velders, A. H. *Inorg. Chem.* **2012**, *51*, 2105−2114.
(19) (a) You, Y.; Han, Y.; Lee, Y.-M.; Park, S. Y.; Nam, W.; Lippard, S. J. *J. Am. Chem. Soc.* **2011**, *133*, 11488−11491. (b) Wu, Y.; Jing, H.; Dong, Z.; Zhao, Q.; Wu, H.; Li, F. *Inorg. Chem.* **2011**, *50*, 7412−7420.
(20) (a) Yoshihara, T.; Karasawa, Y.; Zhang, S.; Hosaka, M.; Takeuchi, T.; Iida, Y.; Endo, K.; Imamura, T.; Tobita, S. *Proc. SPIE-Int. Soc. Opt. Eng.* **2009**, *7190*, 71900× 1−71900 × 8. (b) Zhang, S.; Hosaka, M.; Yoshihara, T.; Negishi, K.; Iida, Y.; Tobita, S.; Takeuchi, T. *Cancer Res.* **2010**, *70*, 4490−4498.
(21) For other metal complexes that respond to hypoxia in tissues: (a) Rumsey, W. L.; Vanderkooi, J. M.; Wilson, D. F. *Science* **1988**, *241*, 1649−1651. (b) Wilson, D. F.; Cerniglia, G. J. *Cancer Res.* **1992**, *52*, 3988−3993. (c) Lebedev, A. Y.; Cheprakov, A. V.; Sakadžić., S.; Boas, D. A.; Wilson, D. F.; Vinogradov, S. A. *ACS Appl. Mater. Interfaces* **2009**, *1*, 1292−1304.
(22) (a) Sharman, W. M.; Allen, C. M.; van Lier, J. E. *Drug Discovery Today* **1999**, *4*, 507−517. (b) Castano, A. P.; Demidova, T. N.; Hamblin, M. R. *Photodiagn. Photodyn. Ther.* **2004**, *1*, 279−293. (c) Wilson, B. C.; Patterson, M. S. *Phys. Med. Biol.* **2008**, *53*, R61−R109. (d) Celli, J. P.; Spring, B. Q.; Rizvi, I.; Evans, C. L.; Samkoe, K. S.; Verma, S.; Pogue, B. W.; Hasan, T. *Chem. Rev.* **2010**, *110*, 2795−2838.
(23) (a) Ali, H.; van Lier, J. E. *Chem. Rev.* **1999**, *99*, 2379−2450. (b) DeRosa, M. C.; Crutchley, R. J. *Coord. Chem. Rev.* **2002**, *233*−*234*, 351−357. (c) Gorman, A.; Killoran, J.; O'Shea, C.; Kenna, T.; Gallagher, W. M.; O'Shea, D. F. *J. Am. Chem. Soc.* **2004**, *126*, 10619−10631. (d) Yogo, T.; Urano, Y.; Mizushima, A.; Sunahara, H.; Inoue, T.; Hirose, K.; Iino, M.; Kikuchi, K.; Nagano, T. *Proc. Natl. Acad. Sci. U.S.A.* **2008**, *105*, 28−32. (e) Chen, Y.; Zheng, W.; Li, Y.; Zhong, J.; Ji, J.; Shen, P. *Cancer Sci.* **2008**, *99*, 2019−2027. (f) Panzarini, E.; Tenuzzo, B.; Dini, L. *Ann. N.Y. Acad. Sci.* **2009**, *1171*, 617−626. (g) Lovell, J. F.; Liu, T. W. B.; Chen, J.; Zheng, G. *Chem. Rev.* **2010**, *110*, 2839−2857. (h) Olivo, M.; Du, H.-Y.; Bay, B.-H. *Curr. Clin. Pharmacol.* **2006**, *1*, 217−222.
(24) (a) Gao, R.; Ho, D. G.; Hernandez, B.; Selke, M.; Murphy, D.; Djurovich, P. I.; Thompson, M. E. *J. Am. Chem. Soc.* **2002**, *124*, 14828−14829. (b) Djurovich, P. I.; Murphy, D.; Thompson, M. E.;

Hernandez, B.; Gao, R.; Hunt, P. L.; Selke, M. *Dalton Trans.* **2007**, 3763−3770. (c) Takizawa, S.; Aboshi, R.; Murata, S. *Photochem. Photobiol. Sci.* **2011**, *10*, 895−903. (d) Sun, J.; Zhao, J.; Guo, H.; Wu, W. *Chem. Commun.* **2012**, *48*, 4169−4171. (e) Lai, C.-W.; Wang, Y.-H.; Lai, C.-H.; Yang, M.-J.; Chen, C.-Y.; Chou, P.-T.; Chan, C.-S.; Chi, Y.; Chen, Y.-C.; Hsiao, J.-K. *Small* **2008**, *4*, 218−224.

(25) (a) Bonneau, R.; Pottier, R.; Bagno, O.; Joussot-Dubien, J. *Photochem. Photobiol.* **1975**, *21*, 159−163. (b) Pottier, R.; Bonneau, R.; Joussot-Dubien, J. *Photochem. Photobiol.* **1975**, *22*, 59−61. (c) McDonnell, S. O.; Hall, M. J.; Allen, L. T.; Byrne, A.; Gallagher, W. M.; O'Shea, D. F. *J. Am. Chem. Soc.* **2005**, *127*, 16360−16361. (d) Arnbjerg, J.; Johnsen, M.; Nielsen, C. B.; Jørgensen, M.; Ogilby, P. R. *J. Phys. Chem. A* **2007**, *111*, 4573−4583.

(26) Aoki, S.; Matsuo, Y.; Ogura, S.; Ohwada, H.; Hisamatsu, Y.; Moromizato, S.; Shiro, M.; Kitamura, M. *Inorg. Chem.* **2011**, *50*, 806−818.

(27) Hisamatsu, Y.; Aoki, S. *Eur. J. Inorg. Chem.* **2011**, 5360−5369.

(28) Zhow and Müllen reported on the iodonization of Ir complex for the synthesis of dendrimers having Ir complex cores, see: Qin, T.; Ding, J.; Wang, L.; Baumgarten, M.; Zhou, G.; Müllen, K. *J. Am. Chem. Soc.* **2009**, *131*, 14329−14336.

(29) Frisch, M. J.; Trucks, G. W.; Schlegel, H. B.; Scuseria, G. E.; Robb, M. A.; Cheeseman, J. R.; Montgomery, J. A.; Vreven, Jr., T.; Kudin, K. N.; Burant, J. C.; Millam, J. M.; Iyengar, S. S.; Tomasi, J.; Barone, V.; Mennucci, B.; Cossi, M.; Scalmani, G.; Rega, N.; Petersson, G. A.; Nakatsuji, H.; Hada, M.; Ehara, M.; Toyota, K.; Fukuda, R.; Hasegawa, J. Ishida, M.; Nakajima, T.; Honda, Y.; Kitao, O.; Nakai, H.; Klene, M.; Li, X.; Knox, J. E.; Hratchian, H. P.; Cross, J. B.; Bakken, V.; Adamo, C.; Jaramillo, J.; Gomperts, R.; Stratmann, R. E.; Yazyev, O.; Austin, A. J.; Cammi, R.; Pomelli, C.; Ochterski, J. W.; Ayala, P. Y.; Morokuma, K.; Voth, G. A.; Salvador, P.; Dannenberg, J. J.; Zakrzewski, V. G.; Dapprich, S.; Daniels, A. D.; Strain, M. C.; Farkas, O.; Malick, D. K.; Rabuck, A. D.; Raghavachari, K.; Foresman, J. B.; Ortiz, J. V.; Cui, Q.; Baboul, A. G.; Clifford, S.; Cioslowski, J.; Stefanov, B. B.; Liu, G.; Liashenko, A.; Piskorz, P.; Komaromi, I.; Martin, R. L.; Fox, D. J.; Keith, T.; Al-Laham, M. A.; Peng, C. Y.; Nanayakkara, A.; Challacombe, M.; Gill, P. M. W.; Johnson, B.; Chen, W.; Wong, M. W.; Gonzalez, C.; Pople, J. A. *Gaussian 03*, Revision C.02; Gaussian, Inc.: Wallingford, CT, 2004.

(30) (a) Kimura, E.; Aoki, S.; Kikuta, E.; Koike, T. *Proc. Natl. Acad. Sci. U.S.A.* **2003**, *100*, 3731−3736. (b) Kimura, E.; Takasawa, R.; Tanuma, S.; Aoki, S. *Sci. STKE* **2004**, *2004*, 7 , and references cited therein.

(31) UV/vis and luminescent spectra of **5** were measured in degassed DMSO at 298 K. UV/vis spectra of acid-free **5** and H_3·**5** in DMSO and DMSO/buffer solution are shown in Figure S1 and S2 in the Supporting Information, and photochemical properties of acid-free **5** and H_3·**5** are summarized in Table S2 in the Supporting Information, respectively.

(32) Emission decay curves of **5** in DMSO/100 mM buffer (at pH 6.0 and 7.4) are presented in Figure S4 in the Supporting Information. pH-Dependent emission intensity and lifetime of **5** at pH 6.0 and 7.4 are shown in Figure S5.

(33) The $\tau^{1/2}$ values of acid-free **5**, H·**5**, H_2·**5**, and H_3·**5** are 2.9 μs, 2.7 μs, 2.0 μs, and 1.5 μs in DMSO (**5** was acidified with HCl in 1,4-dioxane). Figure S5 in the Supporting Information shows comparison of pH-dependent change in emission intensity of **5** (excitation at 366 nm and emission at 494 nm) and pH-dependent change in lifetime of **5**, indicating that these two curves are almost superimposable.

(34) TD-DFT calculation of monoprotonated, diprotonated, and triprotonated forms of **5**, (H·**5**, H_2·**5**, and H_3·**5**) was also conducted and these results are summarized Figure S9 in the Supporting Information, suggesting that excited states of H·**5** and H_2·**5** include a complicated mixture of ^{3}MLCT, ^{3}LC, ^{3}LLCT, and ^{3}ILCT states.

(35) Growth of HeLa-S3 cells in the absence and presence of Ir complexes, **2**, **4**, and **5** (10 μM) without photoirradiation is shown in Figure S10a in the Supporting Information. It should be noted that only **4** induces cell death after incubation for *4 days*. Figure S10b in the Supporting Information shows the results of MTT assay of HeLa-S3 cells incubated with **2**, **4**, and **5** for *16 h*, indicating negligible (**2** and **5**) or weak (**4**) toxicity of these Ir complexes.

(36) (a) Poole, B.; Ohkuma, S. *J. Cell Biol.* **1981**, *90*, 665−669. (b) Demaurex, N.; Furuya, W.; D'Souza, S.; Bonifacino, J. S.; Grinstein, S. *J. Biol. Chem.* **1998**, *273*, 2044−2051. (c) Llopis, J.; McCaffery, J. M.; Miyawaki, A.; Farquhar, M. G.; Tsien, R. Y. *Proc. Natl. Acad. Sci. U.S.A.* **1998**, *95*, 6803−6808.

(37) Buckingham, J. In *Dictionary of Organic Compounds*, 5th ed.; 5th suppl.; Chapman and Hall: London, U.K., 1987.

(38) Confocal images of HeLa-S3 cells dual-staining with **5** (10 μM) and LysoTracker (100 nM) or MitoTracker (10 nM) are shown in Figure S14 in the Supporting Information.

(39) We confirmed that emission of LysoTracker negligibly changes from pH 4 to pH 9. For the reference of lysosome membrane permeability of amines, see: Andrew, C. L.; Klemm, A. R.; Lloyd, J. B. *Biochim. Biophys. Acta* **1997**, *1330*, 71−82.

(40) Dröse, S.; Altendorf, K. *J. Exp. Biol.* **1997**, *200*, 1−8.

(41) It is reported that emission of LysoTracker is lowered in cells treated with concanamycin A. See: Coen, K.; Flannagan, R. S.; Baron, S.; Carraro-Lacroix, L. R.; Wang, D.; Vermeire, W.; Michiels, C.; Munck, S.; Baert, V.; Sugita, S.; Wuytack, F.; Hiesinger, P. R.; Grinstein, S.; Annaert, W. *J. Biol. Chem.* **2012**, *198*, 23−35.

(42) For other detection of $^1O_2$, see: Snyder, J. W.; Skovsen, E.; Lambert, J. D. C.; Ogilby, P. R. *J. Am. Chem. Soc.* **2005**, *127*, 14558−14559.

(43) Howard, J. A.; MendenHall, G. D. *Can. J. Chem.* **1975**, *53*, 2199−2201.

(44) Results of cell membrane swelling upon photoirradiation in the presence of Ir complexes **2**, **4**, **5** and methylene blue are summarized in Table S3 in the Supporting Information.

(45) Galluzzi, L.; Vitale, I.; Abrams, J. M.; Alnemri, E. S.; Baehrecke, E. H.; Blagosklonny, M. V.; Dawson, T. M.; Dawson, V. L.; El-Deiry, W. S.; Fulda, S.; Gottlieb, E.; Green, D. R.; Hengartner, M. O.; Kepp, O.; Knight, R. A.; Kumar, S.; Lipton, S. A.; Lu, X.; Madeo, F.; Malorni, W.; Mehlen, P.; Nuñez, G.; Peter, M. E.; Piacentini, M.; Rubinsztein, D. C.; Shi, Y.; Simon, H.-U.; Vandenabeele, P.; White, E.; Yuan, J.; Zhivotovsky, B.; Melino, G.; Kroemer, G. *Cell Death Differ.* **2012**, *19*, 107−120.

(46) (a) Bursch, W. *Cell Death Differ.* **2001**, *8*, 569−581. (b) Jäättelä, M. *Oncogene* **2004**, *23*, 2746−2756. (c) Guicciardi, M. E.; Leist, M.; Gores, G. J. *Oncogene* **2004**, *23*, 2881−2890. (d) Fehrenbacher, N.; Jäättelä, M. *Cancer Res.* **2005**, *65*, 2993−2995.

(47) For review and foresight of photochemical devices and their applications, see: Garcia-Garibay, M. A. *J. Am. Chem. Soc.* **2012**, *134*, 8289−8292.

(48) Quite recently, Glazer et al. reported the structurally-strained ruthenium complexes as potent light-activated anticancer agents. See: Howerton, B. S.; Heidary, D. K.; Glazer, E. C. *J. Am. Chem. Soc.* **2012**, *134*, 8324−8327.